

AN IMPROVED MASS DETERMINATION FOR M31 FROM ITS SATELLITE GALAXIES

PATRICK CÔTÉ,^{1,2} MARIO MATEO,³ W. L. W. SARGENT,¹ AND EDWARD W. OLSZEWSKI⁴

Received 2000 March 15; accepted 2000 May 19; published 2000 June 28

ABSTRACT

The High-Resolution Echelle Spectrometer on the Keck I telescope has been used to measure the first radial velocities for stars belonging to the Andromeda I and III dwarf spheroidal galaxies. Our radial velocity for And III matches that reported by Blitz & Robishaw for an adjacent H I gas complex, supporting the association of this galaxy with a high-velocity cloud. New and previously published radial velocities for a sample of confirmed or suspected M31 satellites are combined with a homogeneous set of distance estimates to calculate the total mass of M31. Assuming the satellite orbits are isotropic, we find a median mass of $M_A \approx (7.9 \pm 0.5) \times 10^{11} M_\odot$ from eight candidate satellites having deprojected distances from M31 in excess of $R_A \approx 100$ kpc. If the orbits are radial, the inferred mass increases to $M_A \approx (21.5 \pm 3.8) \times 10^{11} M_\odot$; for circular orbits, the enclosed mass is $M_A \approx (3.7 \pm 0.4) \times 10^{11} M_\odot$. These masses are somewhat lower than those found for luminous spiral galaxies based on the ensemble dynamics of their satellites, although the estimates are nevertheless consistent given the large uncertainties.

Subject headings: galaxies: halos — galaxies: individual (M31) — galaxies: kinematics and dynamics — galaxies: spiral — intergalactic medium

1. INTRODUCTION

Although the flat rotation curves of spiral galaxies have firmly established the presence of massive dark halos in these systems, their total masses and spatial extents are still largely unconstrained by H I rotation curves. Aside from a few notable exceptions (e.g., Pickering et al. 1997), the H I disks can only be traced out to distances of a few optical radii. Our understanding of galaxy formation and evolution, of cluster/group dynamics, and of gravitational lensing are limited by this lack of observational constraints.

Attempts to measure the mass and extent of dark halos in spiral galaxies using their associated systems of dwarf galaxies are compromised by the small number of satellites associated with any particular spiral which are bright enough to allow radial velocity measurements. Zaritsky et al. (1993, 1997) have attempted to circumvent this obstacle by accumulating velocities for a small number of companions of many different spiral galaxies and treating the *ensemble* as a single satellite system. While such studies have provided important information on the masses of disk galaxies on scales of a few hundred kiloparsecs, the technique hinges on the key assumption that there exists no connection between the properties of the luminous disk components of spiral galaxies and those of their dark halos.

An obvious alternative approach is to measure velocities for a large number of satellites belonging to one particular spiral galaxy. To date, the only spiral galaxy for which this has been possible is the Milky Way. Such studies, which began with the work of Hartwick & Sargent (1978), provide the most direct observational constraints on the mass of the Galaxy on scales in excess of ~ 100 kpc. Many subsequent efforts have improved on the difficult velocity measurements for these low surface brightness satellites (e.g., Olszewski, Aaronson, & Peterson 1986; Zaritsky et al. 1989) and have refined the statistical tools used to calculate the enclosed mass (e.g., Little & Tremaine

1987; Kochanek 1996). The total mass of the Galaxy inferred from these studies falls in the range of $2.4 \times 10^{11} \leq M/M_\odot \leq 12.5 \times 10^{11}$, where the principal source of uncertainty is whether or not Leo I should be included as a bound member of the Galactic dwarf system.

In this Letter, we apply this technique to a second spiral satellite system—that of M31. While our mass estimate for M31 is not the first to make use of radial velocities for its satellites (see, e.g., van den Bergh 1981), we utilize both new and previously published radial velocities for an expanded sample of known or suspected satellites of M31. In addition, we make use of a homogeneous set of distance determinations for these galaxies in order to pinpoint each object within the M31 halo. From the motions of eight companion galaxies having deprojected distances from M31 in the range of $100 \text{ kpc} \leq R_A \leq 500 \text{ kpc}$, we calculate a total mass of $M_A = 8_{-4}^{+14} \times 10^{11} M_\odot$, where the quoted uncertainties reflect the unknown shapes of the satellite orbits.

2. OBSERVATIONS AND REDUCTIONS

On the night of 1999 August 13, we used the High-Resolution Echelle Spectrometer (HIRES; Vogt et al. 1994) on the Keck I telescope to obtain spectra for two candidate red giant branch (RGB) stars in each of Andromeda I and III, two dwarf spheroidal (dSph) companions of M31. In the case of And I, program stars were selected from the imaging study of Mould & Kristian (1990). For And III, objects were selected using the photometry of Armandroff et al. (1993). The targeted stars were chosen to have magnitudes and colors that place them near the tip of the RGB and to have positions close to the centers of these galaxies.

The instrumental setup and data reduction procedures closely resemble those described in earlier papers (e.g., Vogt et al. 1995; Côté et al. 1999), so we give only a brief description here. The detector was binned 2×2 , giving an effective area of 1024×1024 pixels. A single readout amplifier was employed, adjusted to a gain setting of $2.4 e^- \text{ ADU}^{-1}$. The cross disperser was used in first order to isolate the spectral region $4600 \text{ Å} \leq \lambda \leq 7025 \text{ Å}$, while the C5 dekker was used to limit the entrance aperture to $1''.13 \times 7''.0$. Exposure times for all program stars were 3600 s, with Th-Ar comparison lamp spectra taken im-

¹ California Institute of Technology, MS 105-24, Pasadena, CA 91125.

² Sherman M. Fairchild Fellow.

³ Department of Astronomy, 821 Dennison Building, University of Michigan at Ann Arbor, Ann Arbor, MI 48109.

⁴ Steward Observatory, 933 North Cherry Avenue, University of Arizona, Tucson, AZ 85721-0065.

TABLE 1
HIRES OBSERVATIONS OF RGB STARS IN AND I AND III

Galaxy	Identification ^a	V (mag)	(V-I) (mag)	T (s)	HJD (2,440,000+)	R_{TD}	v_h (km s ⁻¹)
And I	MK087	22.25	1.53	3600	11,405.3662	3.70	-354.3 ± 2.6
	MK344	22.09	1.35	3600	11,405.4123	5.11	-376.2 ± 2.0
And III	A32	22.13	1.41	3600	11,405.4732	3.79	-340.3 ± 2.5
	A28	22.14	2.45	3600	11,405.5253	4.95	-357.3 ± 2.0

^a From Mould & Kristian 1990 and Armandroff et al. 1993.

mediately before and after each exposure. A total of 29 echelle orders were extracted for each program spectrum, although radial velocities were measured using only those five orders which produced the best cross-correlation functions (i.e., two orders spanning the range of $4985 \text{ \AA} \leq \lambda \leq 5125 \text{ \AA}$ and three orders covering the interval of $5285 \text{ \AA} \leq \lambda \leq 5520 \text{ \AA}$). Nine high signal-to-noise ratio spectra for four IAU radial velocity standard stars were also obtained during twilight: HD 161096 (K2 III), HD 182572 (G7 IV), HD 9138 (K4 III), and HD 26162 (K1 III). These spectra were reduced in an identical manner to those of the dSph program stars and were used to create a master template as described in Vogt et al. (1995). A radial velocity for each program star was then derived by cross-correlating its spectra against that of the master template.

Results are presented in Table 1, which gives the identification number, V magnitude, and (V-I) color of each star as well as the exposure time and heliocentric Julian Date of each observation. The Tonry-Davis R_{TD} value of the corresponding cross-correlation function (Tonry & Davis 1979) and the measured heliocentric radial velocity are recorded in the final two columns. Velocity uncertainties have been calculated as described in Côté et al. (1999). For both galaxies, the two program stars have similar radial velocities, suggesting that all four program stars are bona fide members of their respective galaxies.⁵ Thus, our adopted heliocentric radial velocities for And I and III are $v_h = -368 \pm 11$ and $-351 \pm 9 \text{ km s}^{-1}$, respectively, where the uncertainties have been calculated as described by Pryor & Meylan (1993).

3. DISCUSSION

3.1. The dSph-High-Velocity Cloud Connection

Blitz & Robishaw (2000) have identified a high-velocity cloud (HVC) in close proximity to And III. Based on this spatial coincidence, they argued that this H I cloud, which has a heliocentric radial velocity $v_h = -341 \pm 6 \text{ km s}^{-1}$, is physically associated with this galaxy. Their conclusion is supported by the observations presented here since the optical and H I velocities differ by only $\Delta v_h = 10 \pm 11 \text{ km s}^{-1}$, strengthening the case for substantial gaseous components in at least some Local Group dSph galaxies (Carignan et al. 1998; Blitz & Robishaw 2000).

In the case of And I, Blitz & Robishaw (2000) found marginal evidence for an HVC having a heliocentric radial velocity $v_h \sim -300 \text{ km s}^{-1}$. Deeper observations, however, did not confirm this H I feature, and the authors regarded this result as a nondetection. Our HIRES radial velocity differs significantly (i.e., $\Delta v_h = 68 \text{ km s}^{-1}$) from the provisional value of Blitz & Robishaw (2000).

⁵ Note that solar reflex motion in the direction of M31 is $\approx -174 \text{ km s}^{-1}$.

3.2. The Mass of M31

Several features of the M31 satellite system make it an attractive candidate for studying the large-scale distribution of dark matter. First, the sample of known or suspected companions is large compared with other spiral galaxies (and is exceeded only by that of the Milky Way). Second, with efficient spectrographs on 10 m-class telescopes, accurate radial velocity measurements are possible for even the faintest systems. Third, the system's proximity and large spatial extent allow deprojected distances from M31 to be calculated on an object-by-object basis since accurate and homogeneous distances are now available for most of the satellites.

We calculate the deprojected distance from M31, R_A , for each galaxy by combining the projected distance, R_p , with the measured difference along the line of sight, $R_L = D - D_A \cos \Omega_A$, where Ω_A is the angular distance from M31. Whenever possible, we adopt distance determinations based on the tip of the RGB (TRGB) method. With the exception of M32, all of the known or suspected satellites of M31 have distances derived from this method (or, in a few cases, on a related indicator: isochrone fitting of the RGB). For M32, no TRGB distance is available, so we assume the galaxy is located at the same distance as M31, as suggested by several other distance indicators (see, e.g., Grillmair et al. 1996, Ferrarese et al. 2000, and references therein). We adopt a distance of $D_A = 780 \pm 25 \text{ kpc}$ for M31, based on isochrone fits to the RGBs of its globular clusters (Holland 1998). This corresponds to a distance modulus of $(m-M)_0 = 24.46 \text{ mag}$.

Data for 12 confirmed or suspected satellites of M31 are presented in Table 2. From left to right, this table records the galaxy name, Galactic longitude and latitude, adopted distance, projected separation from M31, distance from M31 along the line of sight, the resulting deprojected distance from M31, heliocentric radial velocity, and radial velocity in a frame in which M31 is at rest. Three estimates for the enclosed M31 mass, calculated as described below for isotropic, radial, and circular orbits, are presented in the next three columns. References for the adopted distances and velocities of the satellites are given in the final column. Note that Table 2 contains several Local Group galaxies (i.e., M33, LGS 3, IC 10, Pegasus, and IC 1613) with $R_A \geq 200 \text{ kpc}$. It is not clear which, if any, of these galaxies are bona fide M31 satellites (particularly IC 1613, which is located at a projected distance of $R_p \sim 0.5 \text{ Mpc}$ from M31). These galaxies have been included in the following analysis in order to assess the likelihood of their membership in the M31 subsystem of the Local Group.

For each galaxy, we calculate the line-of-sight velocity in a frame that is at rest with respect to M31 (e.g., Lynden-Bell 1999):

$$v_A = v_h + 9 \cos b \cos l + 232 \cos b \sin l + 7 \sin b + 123 \cos \Omega_A. \quad (1)$$

TABLE 2
DATA FOR CANDIDATE SATELLITES OF M31

GALAXY	l (deg)	b (deg)	D (kpc)	R_p (kpc)	R_L (kpc)	R_A (kpc)	v_h (km s ⁻¹)	v_A (km s ⁻¹)	$M_A(\text{iso})$ ($\times 10^{11} M_\odot$)	$M_A(\text{rad})$ ($\times 10^{11} M_\odot$)	$M_A(\text{cir})$ ($\times 10^{11} M_\odot$)	REFERENCES	
												D^a	v^b
NGC 147	119.8	-14.3	755 \pm 17	101	-18	103 ⁺⁴ ₋₂	-193 \pm 3	118 \pm 3	9.8 ^{+0.9} _{-0.6}	205 ⁺²⁰ ₋₁₃	3.4 ^{+0.7} _{-0.3}	1	2
NGC 185	120.8	-14.5	620 \pm 60	96	-154	182 ⁺⁵³ ₋₄₇	-202 \pm 3	107 \pm 3	14.2 ^{+5.2} _{-4.3}	13.4 ^{+4.9} _{-4.0}	17.1 ^{+21.9} _{-10.5}	3	2
And III	119.3	-26.2	760 \pm 70	68	-17	70 ⁺⁴¹ ₋₂	-351 \pm 9	-54 \pm 9	1.4 ^{+1.6} _{-0.5}	15.8 ^{+18.2} _{-5.2}	0.5 ^{+2.2} _{-0.2}	4	5
NGC 205	120.7	-21.1	830 \pm 115	8	50	51 ⁺¹¹⁵ ₋₄₂	-241 \pm 3	61 \pm 3	1.3 ^{+3.4} _{-1.1}	0.9 ^{+2.4} _{-0.8}	16.4 ⁺⁶⁰⁸ _{-16.3}	6	2
M32	121.2	-22.0	780 \pm 25 ^c	6	0	6 ⁺²⁰ ₋₁	-200 \pm 6	100 \pm 6	0.39 ^{+1.63} _{-0.05}	...	0.13 ^{+14.37} _{-0.02}	7	
And I	121.7	-24.9	790 \pm 25	45	11	46 ⁺¹¹ ₋₂	-368 \pm 11	-73 \pm 11	1.7 ^{+1.1} _{-0.5}	19.2 ^{+12.5} _{-5.8}	0.6 ^{+1.0} _{-0.2}	8	5
LGS 3	126.8	-40.9	810 \pm 80	265	76	276 ⁺³² ₋₁₁	-282 \pm 4	-35 \pm 4	2.0 ^{+0.8} _{-0.5}	20.0 ^{+7.8} _{-5.0}	0.8 ^{+0.6} _{-0.3}	9	10
And II	128.9	-29.2	680 \pm 19	140	-87	165 ⁺¹¹ ₋₉	-188 \pm 3	82 \pm 3	7.5 ^{+1.1} _{-0.9}	18.4 ^{+2.7} _{-2.3}	3.6 ^{+1.1} _{-0.1}	8	11
IC 10	119.0	-3.3	660 \pm 63	245	-80	258 ⁺²⁶ ₋₁₂	-348 \pm 1	-33 \pm 1	1.8 ^{+0.3} _{-0.2}	13.9 ^{+2.3} _{-1.4}	0.7 ^{+0.3} _{-0.1}	12	7
IC 1613	129.8	-60.6	715 \pm 40	496	113	508 ⁺¹⁰ ₋₇	-234 \pm 1	-60 \pm 1	7.7 ^{+0.5} _{-0.4}	176 ⁺¹⁰ ₋₈	4.5 ^{+0.4} _{-0.3}	13	7
M33	133.6	-31.3	870 \pm 32	199	116	230 ⁺¹⁸ ₋₁₄	-180 \pm 1	74 \pm 1	8.1 ^{+0.9} _{-0.7}	22.9 ^{+2.4} _{-2.0}	3.9 ^{+1.1} _{-0.8}	14, 15	7
Pegasus	94.8	-43.6	760 \pm 100	402	92	412 ⁺³³ ₋₁₀	-183 \pm 2	84 \pm 2	15.1 ^{+2.1} _{-1.1}	278 ⁺³⁷ ₋₂₀	7.2 ^{+2.3} _{-0.8}	16	17

^a References for distance.

^b References for velocities.

^c Assumed to lie at our adopted M31 distance of $D_A = 780 \pm 25$ kpc (Holland 1998).

REFERENCES.—(1) Han et al. 1997; (2) Bender, Paquet, & Nieto 1991; (3) Lee, Freedman, & Madore 1993; (4) Armandroff et al. 1993; (5) This Letter; (6) Lee 1996; (7) Huchra, Vogeley, & Geller 1999; (8) Da Costa et al. 2000; (9) Lee 1995; (10) Cook et al. 1999; (11) Côté et al. 1999; (12) Sakai, Madore, & Freedman 1999; (13) Cole et al. 1999; (14) Mould & Kristian 1986; (15) Ferrarese et al. 2000; (16) Gallagher et al. 1998; (17) Lu et al. 1993.

If we approximate the satellite system as a spherical collection of test particles that are bound to a massive central object, then, for an assumed isotropic velocity distribution, the mass of M31 is simply

$$M_A = 3v_{\parallel}^2 R_A / G, \quad (2)$$

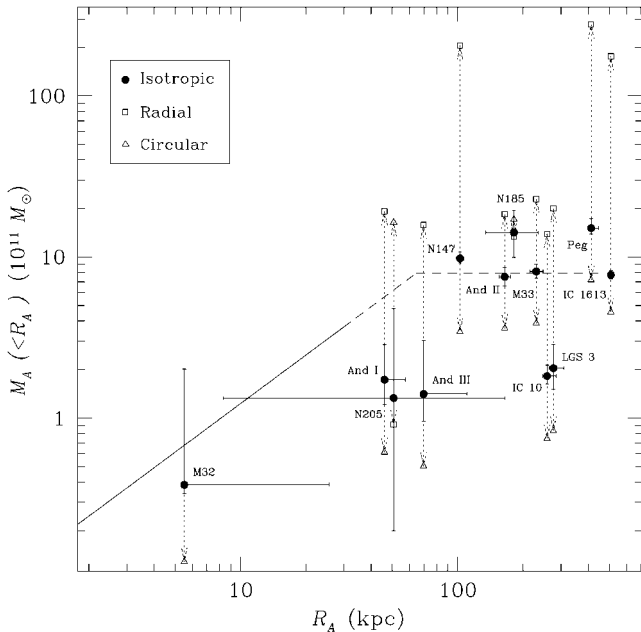


FIG. 1.—Enclosed mass plotted as a function of deprojected distance from M31 for the candidate satellites given in Table 2. The filled circles and error bars refer to mass estimates based on the assumption that the satellite system has a isotropic velocity dispersion tensor; the arrows indicate the change in the calculated mass if the satellites are assumed to move along radial or circular orbits (squares and triangles, respectively). The solid line shows the enclosed mass calculated from the observed rotation curve, $M_A = v_c^2 R_A / \sin^2 i G$, where $v_c = 230$ km s⁻¹ (Rubin & Ford 1970; Newton & Emerson 1977). For isotropic orbits, the eight galaxies with $R_A \geq 100$ kpc yield a median mass of $M_A \approx (7.9 \pm 0.5) \times 10^{11} M_\odot$, equivalent to that found from extrapolating the rotation curve to $R_A \approx 65$ kpc (dashed line).

where R_A is the deprojected distance from M31 and $v_{\parallel} = v_A \cos \Omega_A$ is the component of v_A parallel to the vector connecting M31 with the Sun. This correction assures that the same component of the space velocity is used for each of the satellites and implicitly assumes that the tangential velocity of M31 can be safely neglected (e.g., see Kahn & Woltjer 1959). On the other hand, if the satellites' orbits are purely radial, then the enclosed mass becomes (e.g., Lynden-Bell, Cannon, & Godwin 1983; Binney & Tremaine 1987, p. 640)

$$M_A = 2v_A^2 R_A^3 / G(R_A^2 - R_p^2). \quad (3)$$

Such a case might be appropriate for distant satellites that formed with small peculiar velocities and then fell toward M31. However, it is unlikely that many of the known dwarf companions of M31 would survive many such close passages; indeed, Grebel (1999) has argued that the known M31 satellites show a preference for polar orbits. In this case, the appropriate mass estimator is

$$M_A = v_A^2 R_A^3 / G R_p^2, \quad (4)$$

where the satellites' orbits are assumed to be circular.

Note that equations (2)–(4) treat M31 as a point mass. While this assumption is certainly not valid for the innermost satellites, it should be reasonable for the more distant objects. For instance, in the case of circular orbits, we have taken $v_c = v_A R_A / R_p$; the eight objects having $R_A \geq 100$ kpc then yield a mean circular velocity of $\langle v_c \rangle^{1/2} = 92$ km s⁻¹. This is much lower than the value of $v_c = 230$ km s⁻¹ found in the inner regions of the galaxy, suggesting that most of M31's mass lies inside this region and supporting the point-mass approximation.

Figure 1 shows the enclosed M31 mass plotted as a function of deprojected distance for each of the galaxies listed in Table 2. Masses found assuming isotropic orbits are indicated by the filled circles. Associated error bars refer to measurement errors only and do not include uncertainties arising from the unknown shapes of the satellite's orbits (which are, not surprisingly, the dominant sources of uncertainty). The vertical arrows illustrate the change in inferred mass if the orbits are

assumed to be either radial⁶ (*open squares*) or circular (*open triangles*).

As expected, it is the most distant satellites that place the most stringent constraints on the total mass of M31. If the satellite orbits are isotropic, then the median mass implied by the eight galaxies having $R_A \geq 100$ kpc is $M_A \approx (7.9 \pm 0.5) \times 10^{11} M_\odot$, where the quoted uncertainty refers to the statistical error in the median. If the satellite orbits are radial, then the same eight galaxies give $M_A \approx (21.5 \pm 3.8) \times 10^{11} M_\odot$. On the other hand, circular orbits for these galaxies would imply $M_A \approx (3.7 \pm 0.4) \times 10^{11} M_\odot$. Note that two distant objects, LGS 3 and IC 10, yield significantly lower masses than the remaining sample of distant galaxies. However, this apparent discrepancy is removed if their orbits are highly eccentric.

How do the above estimates for the mass of M31 compare with those found using other techniques such as globular clusters, the H I rotation curve, and Local Group dynamics? For comparison, mass estimates for M31 based on the motions of its globular clusters fall in the range of $M_A \approx (3\text{--}8) \times 10^{11} M_\odot$ (Hartwick & Sargent 1974; Huchra, Kent, & Brodie 1991; Federici et al. 1993). Although these values are somewhat lower than those found here, the results are nevertheless consistent given the different spatial distributions of the clusters and dwarf galaxies; i.e., the globular clusters with measured velocities have $R_p \lesssim 30$ kpc. Similarly, our estimate for isotropic orbits is equivalent to that found by simply extrapolating the observed rotation curve out to a distance of $R_A \approx 65$ kpc and assuming a constant circular velocity of $v_c = 230 \text{ km s}^{-1}$ (Rubin & Ford 1970; Newton & Emerson 1977). From a dynamical analysis of the distances

and radial velocities of 28 probable Local Group members, Courteau & van den Bergh (1999) find a Local Group virial mass of $M_{\text{LG}} = (2.3 \pm 0.6) \times 10^{12} M_\odot$. Distributing this mass between M31 and the Milky Way according to their circular velocities leads to an M31 mass of $M_A \approx 12 \times 10^{11} M_\odot$, in acceptable agreement with the mass found here.

It is interesting to compare our estimate for the mass of M31 with those for other large spiral galaxies. Zaritsky et al. (1993, 1997) have carried out an ensemble analysis of 69 satellite galaxies associated with luminous, late-type disk galaxies. The mass found here is somewhat lower than the range of $M = (15\text{--}26) \times 10^{11} M_\odot$ that they find for a typical L^* galaxy. However, given the rather large uncertainties in both estimates, the results are nevertheless consistent.

Finally, we note that Evans & Wilkinson (2000) have recently reported a mass of $M = 12.3_{-6}^{+18} \times 10^{11} M_\odot$ for M31 based on a sophisticated analysis of the radial velocities of its globular clusters, planetary nebulae, and satellite galaxies. Restricting their sample to just the satellite galaxies yields a best-fit mass of $M = 8.1 \times 10^{11} M_\odot$. The excellent agreement with our estimate is not entirely surprising, given that the two studies are based on the same data for several satellites. Nevertheless, our analysis, which is based on improved distances and velocities for an expanded sample of satellites, supports their claim for a rather low mass. Clearly, though, the uncertainties in these estimates remain large, and radial velocities for additional outlying satellites (such as And V, VI, and VII) will help us to refine existing constraints on the mass of M31.

P. C. acknowledges the support provided by the Sherman M. Fairchild Foundation. M. M. was partially supported by NSF grant AST 98-20608 during the course of this work. E. W. O. acknowledges NSF grants AST 92-23967 and AST 96-19524.

REFERENCES

- Armandroff, T. E., Da Costa, G. S., Caldwell, N., & Seitzer, P. 1993, *AJ*, 106, 986
- Bender, R., Paquet, A., & Nieto, J.-L. 1991, *A&A*, 246, 349
- Binney, J., & Tremaine, S. 1987, *Galactic Dynamics* (Princeton: Princeton Univ. Press)
- Blitz, L., & Robishaw, T. 2000, *ApJ*, in press (astro-ph/0001142)
- Carignan, C., Beaulieu, S., Côté, S., Demers, S., & Mateo, M. 1998, *AJ*, 116, 1690
- Cole, A. A., et al. 1999, *AJ*, 118, 1657
- Cook, K. H., Mateo, M., Olszewski, E. W., Vogt, S. S., Stubbs, C., & Diercks, A. 1999, *PASP*, 111, 306
- Côté, P., Mateo, M., Olszewski, E. O., & Cook, K. H. 1999, *ApJ*, 526, 147
- Courteau, S., & van den Bergh, S. 1999, *AJ*, 118, 337
- Da Costa, G. S., Armandroff, T. E., Caldwell, N., & Seitzer, P. 2000, *AJ*, 119, 705
- Evans, N. W., & Wilkinson, M. I. 2000, *MNRAS*, in press (astro-ph/0004187)
- Federici, L., Bonoli, F., Ciotti, L., Fusi Pecci, F., Marano, B., Lipovetsky, V. A., Niezvestny, S. I., & Spassova, N. 1993, *A&A*, 274, 87
- Ferrarese, L., et al. 2000, *ApJ*, 529, 745
- Gallagher, C. J., Tolstoy, E., Dohm-Palmer, R. C., Skillman, E. D., Cole, A. A., Hoessel, J. G., Saha, A., & Mateo, M. 1998, *AJ*, 115, 1869
- Grebel, E. K. 1999, in *IAU Symp. 192, The Stellar Content of Local Group Galaxies*, ed. P. Whitelock & R. Cannon (San Francisco: ASP), 447
- Grillmair, C. J., et al. 1996, *AJ*, 112, 1975
- Han, M., Hoessel, J. G., Gallagher, J. S., III, Holtsman, J., & Stetson, P. B. 1997, *AJ*, 113, 1001
- Hartwick, F. D. A., & Sargent, W. L. W. 1974, *ApJ*, 190, 283
- . 1978, *ApJ*, 221, 512
- Holland, S. 1998, *AJ*, 115, 1916
- Huchra, J. P., Kent, S. M., & Brodie, J. P. 1991, *ApJ*, 370, 495
- Huchra, J. P., Vogeley, M. S., & Geller, M. J. 1999, *ApJS*, 121, 287
- Kahn, F., & Woltjer, L. 1959, *ApJ*, 130, 705
- Kochanek, C. S. 1996, *ApJ*, 457, 228
- Lee, M. G. 1995, *AJ*, 110, 1129
- . 1996, *AJ*, 112, 1438
- Lee, M. G., Freedman, W., & Madore, B. F. 1993, *AJ*, 106, 964
- Little, B., & Tremaine, S. 1987, *ApJ*, 320, 493
- Lu, N. Y., Hoffman, G. L., Groff, T., Roos, T., & Lamphier, C. 1993, *ApJS*, 88, 383
- Lynden-Bell, D. 1999, in *IAU Symp. 192, The Stellar Content of Local Group Galaxies*, ed. P. Whitelock & R. Cannon (San Francisco: ASP), 39
- Lynden-Bell, D., Cannon, R. D., & Godwin, P. J. 1983, *MNRAS*, 204, 87P
- Mould, J., & Kristian, J. 1986, *ApJ*, 305, 591
- . 1990, *ApJ*, 354, 438
- Newton, K., & Emerson, D. T. 1977, *MNRAS*, 181, 573
- Olszewski, E. W., Aaronson, M., & Peterson, R. C. 1986, *ApJ*, 302, L45
- Pickering, T. E., Impey, C. D., van Gorkom, J. H., & Bothun, G. D. 1997, *AJ*, 114, 1858
- Pryor, C., & Meylan, G. 1993, in *ASP Conf. Ser. 50, The Structure and Dynamics of Globular Clusters*, ed. S. G. Djorgovski & G. Meylan (San Francisco: ASP), 357
- Rubin, V. C., & Ford, W. K. 1970, *ApJ*, 159, 379
- Sakai, S., Madore, B. F., & Freedman, W. L. 1999, *ApJ*, 511, 671
- Tonry, J., & Davis, M. 1979, *AJ*, 84, 1511
- van den Bergh, S. 1981, *PASP*, 93, 428
- Vogt, S. S., et al. 1994, *Proc. SPIE*, 2198, 362
- Vogt, S. S., Mateo, M., Olszewski, E. W., & Keane, M. J. 1995, *AJ*, 109, 151
- Zaritsky, D., Olszewski, E. W., Schommer, R. A., Peterson, R. C., & Aaronson, M. 1989, *ApJ*, 345, 759
- Zaritsky, D., Smith, R., Frenk, C., & White, S. D. M. 1993, *ApJ*, 405, 464
- . 1997, *ApJ*, 478, 39